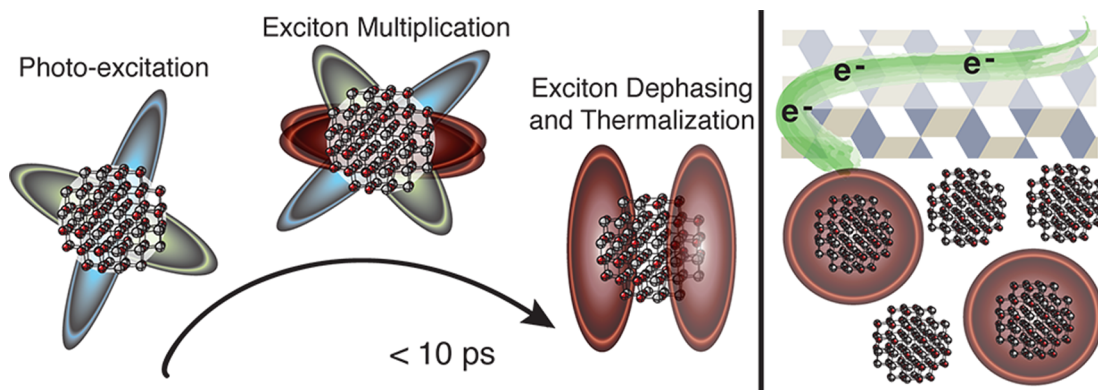# Exciton Multiplication from First Principles

HEATHER M. JAEGER,[†] KIM HYEON-DEUK,[‡] AND
OLEG V. PREZHDO[*, †]

[†]*Department of Chemistry, University of Rochester, Rochester, New York 14627,
United States , and* [‡]*Department of Chemistry, Kyoto University, 606-8502,
Kyoto, Japan*

CONSPECTUS

Third-generation photovolatics require demanding cost and power conversion efficiency standards, which may be achieved through efficient exciton multiplication. Therefore, generating more than one electron—hole pair from the absorption of a single photon has vast ramifications on solar power conversion technology. Unlike their bulk counterparts, irradiated semiconductor quantum dots exhibit efficient exciton multiplication, due to confinement-enhanced Coulomb interactions and slower nonradiative losses. The exact characterization of the complicated photoexcited processes within quantum-dot photovoltaics is a work in progress. In this Account, we focus on the photophysics of nanocrystals and investigate three constituent processes of exciton multiplication, including photoexcitation, phonon-induced dephasing, and impact ionization. We quantify the role of each process in exciton multiplication through ab initio computation and analysis of many-electron wave functions.

The probability of observing a multiple exciton in a photoexcited state is proportional to the magnitude of electron correlation, where correlated electrons can be simultaneously promoted across the band gap. Energies of multiple excitons are determined directly from the excited state wave functions, defining the threshold for multiple exciton generation. This threshold is strongly perturbed in the presence of surface defects, dopants, and ionization.

Within a few femtoseconds following photoexcitation, the quantum state loses coherence through interactions with the vibrating atomic lattice. The phase relationship between single excitons and multiple excitons dissipates first, followed by multiple exciton fission. Single excitons are coupled to multiple excitons through Coulomb and electron-phonon interactions, and as a consequence, single excitons convert to multiple excitons and vice versa. Here, exciton multiplication depends on the initial energy and coupling magnitude and competes with electron—phonon energy relaxation. Multiple excitons are generated through impact ionization within picoseconds.

The basis of exciton multiplication in quantum dots is the collective result of photoexcitation, dephasing, and nonadiabatic evolution. Each process is characterized by a distinct time-scale, and the overall multiple exciton generation dynamics is complete by about 10 ps. Without relying on semiempirical parameters, we computed quantum mechanical probabilities of multiple excitons for small model systems. Because exciton correlations and coherences are microscopic, quantum properties, results for small model systems can be extrapolated to larger, realistic quantum dots.

Introduction

Absorbing a single solar photon, semiconductor quantum dots (QDs)[1−3] generate more than one electron—hole pair.

Efficient exciton multiplication improves the performance of QD solar cells, which potentially meet the demanding cost and power conversion efficiency standards of

third-generation photovoltaics.[4] Additional dynamic processes, including electron transfer, thermalization, and charge carrier recombination, determine the overall output of a photovoltaic device. In order to reap the benefits of QD architectures in solar cells, the rate of exciton or charge carrier multiplication must be faster than competing processes.[5,6]

Physical properties of semiconducting nanocrystals can be associated with either quantum-confined semiconductors or extremely large molecules.[7,8] Charge carriers and carrier multiplication are terms often given to nonequilibrium, bulk-phase semiconductors, where the mechanism of multiplication is impact ionization. Here, impact ionization refers to the process of promoting an electron across the band gap by way of free-carrier collisions. Unlike semiconductors, the photophysics of molecular systems cannot be fully described by independent particles (electrons and holes). The appearance of discrete states in the luminescence spectra of QDs[9,10] confirms that excitons, or bound electron−hole pairs, are generated upon photoexcitation. Large excitonic effects are associated with strong electron−electron interactions and the breakdown of the independent-particle picture in photoexcited QDs. Nanocrystals subject to such strong Coulombic interactions carry a finite probability for the simultaneous excitation of more than one electron across the band gap.[11] In order to distinguish impact ionization in bulk semiconductors from the processes occurring in finite systems and to emphasize the excitonic nature of excited states, carrier multiplication in QDs and molecular systems is often termed multiple exciton generation (MEG).[12]

Multiple excitons (MEs) have been detected in a number of nanocrystals, including PbSe,[13−16] PbS,[14,16] PbTe,[17] CdSe,[16] and Si.[18,19] Femtosecond transient absorption and transient fluorescence techniques allow one to characterize MEG yields and time scales. The signature of MEs typically appears as the change in absorption, or emission, at the energy of the lowest exciton (first excited state). The change is proportional to the number of excitons generated. Sensitive to both sample preparation and data interpretation, these spectroscopic investigations have caused wildly disparate reports on exciton yields in QDs.[20,21] Experimental techniques have progressed in conjunction with a theoretical framework[14,22,23] to show that, as a consequence of enhanced Coulombic interactions, the MEG threshold is slightly above twice the energy of the lowest exciton (E_g). Arrays of silicon QDs generate MEs at excitation energies near $2E_g$ (3.1 eV),[19] which places the MEG threshold within the solar spectrum. Lower band gap materials, such as PbSe,
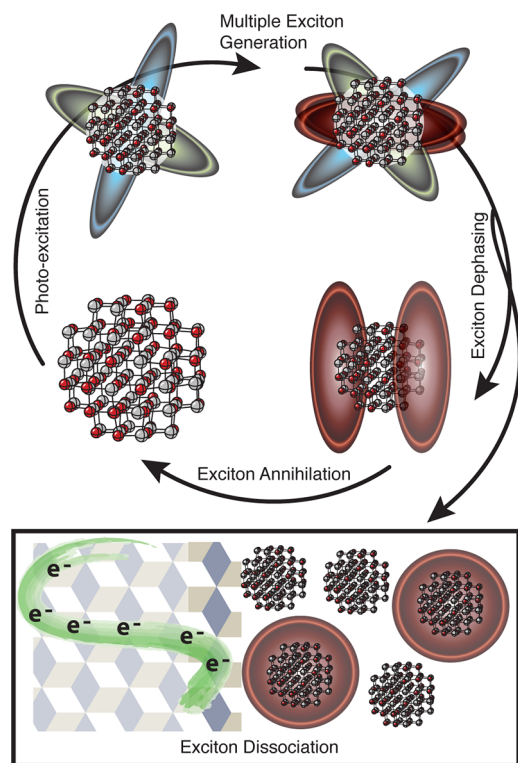

FIGURE 1. Exciton multiplication in a photovoltaic device.

create the possibility of MEG over a larger portion of the solar spectrum. A qualitative overview on the processes of MEG in QD photovoltaics is given in Figure 1.

MEs appear within 100 fs of photoexcitation and persist for tens to hundreds of picoseconds.[24] The ultrafast component of MEG (<100 fs) results from a coherent excitation of more than one electron, due to strong many-body interactions in the excited state. Semiconductor nanocrystals exhibit enhanced Coulombic interactions as well as quasi-continuous band structure. As a consequence of a large density of states, exciton multiplication can also occur through impact ionization, similar to bulk materials.[25] Impact ionization is slower than coherent MEG and spans many orders of magnitude depending on excitation energy and system size.[26,27]

Spectroscopic signals provide raw evidence of carrier multiplication, exciton recombination, and thermalization in photoexcited QDs. Details regarding mechanisms and rates of these processes are further elucidated through theoretical studies. Both theory and experiment agree that impact ionization is too inefficient in bulk semiconductors to significantly benefit solar power conversion efficiencies.[28] Carrier multiplication in bulk silicon becomes competitive at photon energies of ∼4 eV,[18] pushing the limits of the solar spectrum. QDs, through MEG and slower exciton relaxation,
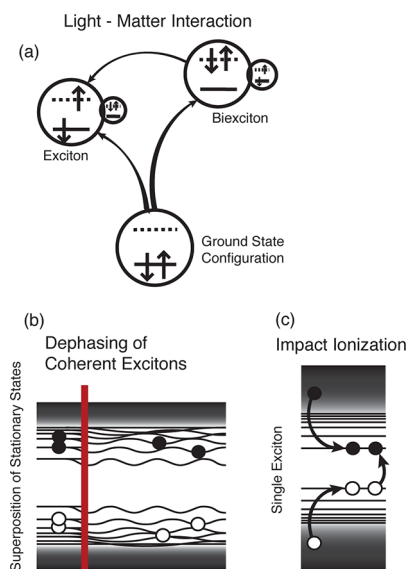
FIGURE 2. (a) Doubly excited configurations provide a quantitative measure of observing MEs in the photoexcited state. (b) Lattice vibrations induce dephasing of superpositions of single and multiple excitons. (c) Energy is transferred from a high-energy exciton to promote an additional electron across the band gap.

provide a route to carrier multiplication in solar cells, as best evidenced by a photon-to-current efficiency exceeding 100%.[29,30]

Ab Initio Simulations of MEG

QDs are composed of hundreds of atoms and tens of thousands of electrons. Computing the exact many-particle wave function of such a system is an arguably impossible task, but, fortunately, an unnecessary one. Using physically motivated approximations and model systems, one can extract meaningful information without reliance on intractable methodology or empirical parameters. The simulations described below treat many-body interactions in the electronic degrees of freedom for either fixed nuclear positions or nuclei undergoing classical motion. Using quantum chemical techniques, wave functions and electronic densities are computed in a basis of electronic configurations and are tethered to the classical nuclei through electron–phonon coupling. Single exciton (SE) and ME states are characterized by both static and dynamic representations of photoexcited QDs. Three key elements to exciton multiplication are illustrated in Figure 2 and described in detail below.

A. Light–Matter Interaction. When QDs absorb light, electrons gain energy and rearrange into higher energy configurations. A ground state configuration differs from excited states by the presence of excitons. Generally, the method of configuration interaction (CI) describes excited states as a superposition of all possible excitations from the Hartree–Fock ground state, Figure 2a. The extent to which doubly excited and higher-ordered configurations enter the wave function reflects the deviation of the excited state from a mean-field representation (dynamic electron correlation) and the probability that MEs are produced during photoexcitation.

By relating singly excited configurations to SEs and doubly excited configurations to MEs, quantum probabilities of observing SEs and MEs in the photoexcited state are calculated from the sum of squares of CI coefficients. Densities of SEs and MEs are determined by multiplying the total density of states (DOS) by the probability of observing an SE or ME. Computed oscillator strengths for each ground to excited state transition associate MEG to the optical response of QDs. Our approach describes exciton generation and photo-induced exciton multiplication for fixed nuclei, neglecting the much slower atomic motions. As the excitation energy increases, the density of MEs increases as well. Thresholds for MEG are found from inspection of ME DOS and optical absorption spectra. These thresholds directly correspond to the onset of MEG deduced from transient absorbance/emission measurements.

B. Dephasing of Coherent Excitons. Coupling between electrons and nuclei results in a modulation of electron/hole energy levels as the lattice undergoes vibrational motion. As a result of disorder in these modulations, electron–phonon interactions induce a loss of phase relationship among coherently excited particles. In less than 100 fs, phonons (lattice vibrations) destroy the quantum mechanical coherences between charge carriers, as shown in Figure 2b. Photoexcited quantum states evolve into independent electrons and holes. Excited states first dephase into SEs and MEs, and, later, MEs undergo a process known as multiple exciton fission (MEF) to generate two (or more) uncorrelated SEs. After phonon-induced MEF, excitons dissociate and become distinct charge carriers.

Unlike thermalization, exciton dephasing does not necessarily involve electron–phonon energy transfer. As an elastic electron–phonon scattering process, pure dephasing conserves energy in the electronic degrees of freedom. Pure dephasing determines the line width associated with homogeneous broadening in optical spectra and can be evaluated through the optical response functions.[31] Employing a quantum-classical representation of phonon-induced dephasing, the energy difference between quantum state constituents, for example, SEs, is monitored over an ensemble of classical trajectories. The amplitude and rate of decay of the energy difference fluctuation determines the

lifetime of the coherent superposition between a quantum state pair.

C. Electron–Phonon Thermalization and Impact Ionization. Immediately following the absorption of a photon, electronic degrees of freedom carry significant excess energy.[5] Bringing the system into thermal equilibrium, the energy is transferred to the lattice by way of electron–phonon coupling. Electronic transitions resonate with phonons, releasing excess energy ($>E_g$) to the environment through phonon emission. Thermalization of electrons and holes in semiconducting nanocrystals takes place in $\sim$10 ps[32,33] and, under the right conditions, suppresses carrier multiplication. Before the electronic energy is lost to phonons, a finite probability exists that a high-energy exciton generates an additional exciton. This Auger-type process, known as impact ionization, happens more easily in QDs, since the Coulomb coupling between electrons and holes is stronger due to confinement.

Exciton dynamics, including electron–phonon relaxation and impact ionization (Figure 2c), can be simulated in the time-domain using time-dependent DFT, where excitons are coupled to phonon motions by means of nonadiabatic molecular dynamics algorithms. Simulations are performed in the adiabatic representation, in which excitons interact through nonadiabatic coupling terms. Adiabatic states are defined as singly and doubly excited electronic configurations with respect to the Kohn–Sham ground state. Purely electronic interactions are embedded in the correlation functional, and nonadiabatic coupling is computed in the independent orbital representation. At every given point along the quantum-classical trajectory, the probability of observing an ME is given by the total population of doubly excited adiabatic states.

Photogeneration of Multiple Excitons

Computed excited states span an energy range from the first excitation to the first ionization, providing a complete analysis of photogenerated MEs. In realistically sized QDs, this energy range contains thousands of excited states, and even a single, many-electron state poses significant computational challenges. In order to overcome these obstacles, calculations are carried out on model QDs, containing around 10 atoms (Figure 3). As proof of concept, the computed single-particle DOS in the model lead selenide and cadmium selenide clusters exhibits the same maxima and minima as those in 300-atom nanocrystals,[34] and optical spectra on 10-atom silicon clusters agree well with theories designed for macroscopic silicon.[35] From analyses of ab
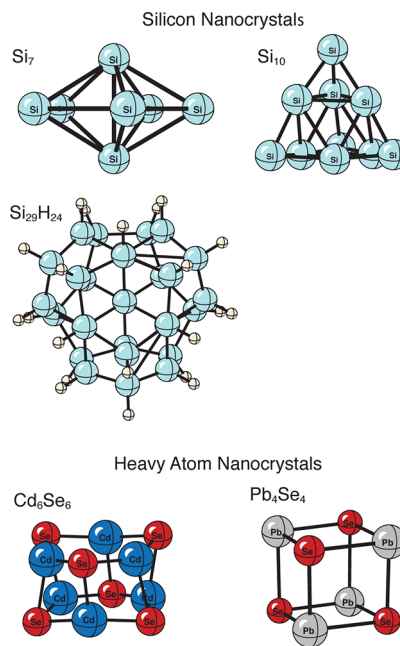

FIGURE 3. Structures of silicon, lead selenide, and cadmium selenide model systems.

initio electronic states, MEG thresholds are determined for ideal lead selenide and silicon QDs[34,36] as well as for ionized and nonstoichiometric forms.[37,38]

A. Ideal Quantum Dots. Both quantum confinement and dielectric screening determine the strength of electron–electron interactions in semiconducting nanocrystals. For QDs with strongly correlated electrons, that is, with radii smaller than the exciton Bohr radius, a_B, and low dielectric constants, one can expect highly efficient MEG via direct generation of MEs. Systems with a large dielectric constant typically have highly delocalized electron–hole pairs. Lead selenide has a dielectric constant of $\sim$23 and $a_B = 47$ nm. Silicon has a dielectric constant of $\sim$12 and $a_B = 4.9$ nm. The much larger a_B of lead selenide gives reason for stronger confinement effects, yet the much larger dielectric constant is indicative of screened interparticle interactions and uncorrelated excitons in the photoexcited state.

Quantum probabilities of observing an ME in Pb_4Se_4 immediately upon photoexcitation are shown in Figure 4. Electronic excitation at energies below $2.5E_g$ predominantly result in SEs. A less than ideal MEG threshold, $2.6E_g$, for a QD free of surface defects suggests that the intrinsic screening of the electronic interactions in lead selenide QDs limits MEG efficiency. As further evidence of uncorrelated excitons, the transition from SEs to MEs over increasing photon energy is extremely sharp: very few states exist that have near equal probabilities of SE and ME generation. In other words,
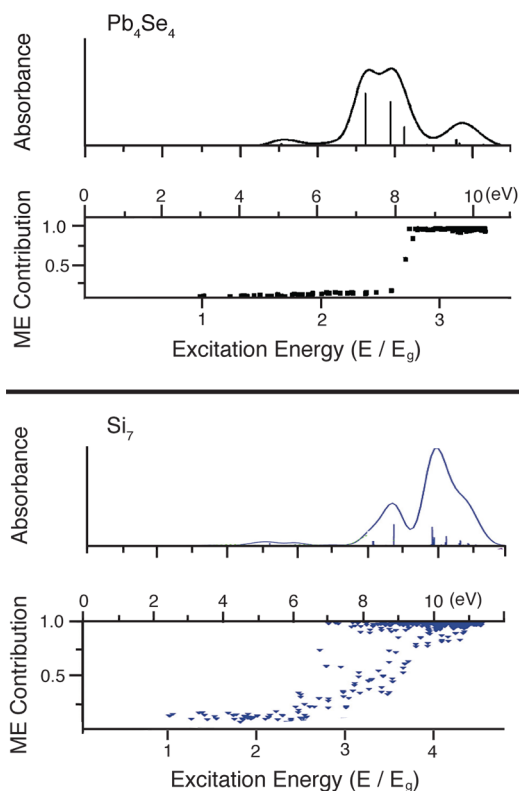
FIGURE 4. Optical spectra and probabilities of observing MEs in photoexcited Pb_4Se_4 (top) and Si_7 (bottom).

FIGURE 5. (top) Excited state wave functions of $Pb_4Se_4{}^+$ are partitioned into contributions from single excitons (SE), multiple excitons (ME), intraband transitions (IB), and a superposition of SEs with IB (SE+IB). (middle, bottom) ME analyses for Pb_3Se_4 and Pb_4Se_3. At low photon energies, electrons are promoted into the gap states (GS).

low-energy SEs in lead selenide QDs rarely induce exciton multiplication through Coulombic interactions, despite significant quantum confinement. Once excitation energies exceed $2.6E_g$, SEs no longer exist independently, and the excited state density takes on significant ME character. Most of the oscillator strength is carried by transitions at the MEG threshold and below (Figure 6). The weaker optical response in the ME states can be attributed to the independent-particle selection rules stating that only one electron can be excited by photon. Nevertheless, absorbance in the ME energy range is strong enough to allow MEG by photoexcitation.

Analyses of the excited state wave functions of Si_7 reveal a qualitatively different perspective of MEG. A large number of electronic states, within the range of 2.4 and $4.0E_g$, are classified as strongly correlated SEs, for which the probability of generating an ME is greater than 30%. The electronic spectrum and ME analysis for Si_7 is presented in the lower panel of Figure 4. The strongly mixed character of the photoexcited states in silicon QDs is indicative of unscreened many-body interactions. Computations of excited states described by singly and doubly excited configurations give an MEG threshold of $\sim 2.4E_g$. By extending CI to higher-ordered configurations, which correlate MEs and
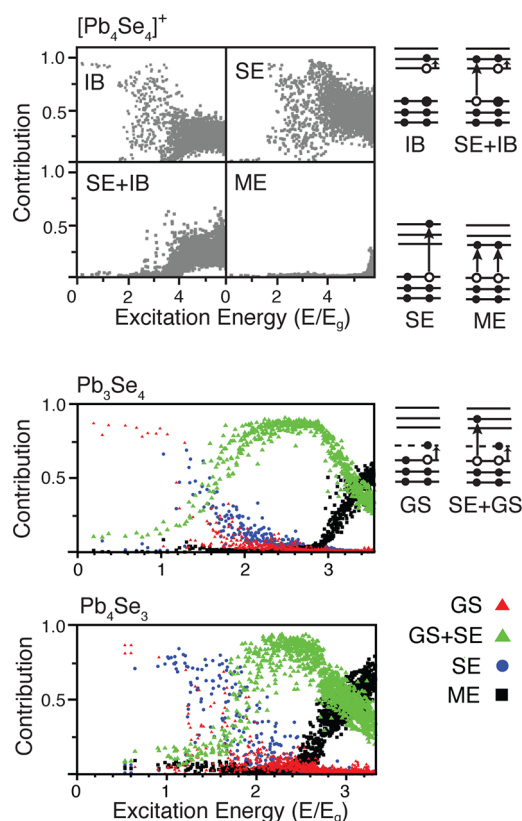
lower the electronic energy, the MEG threshold is reduced.[36] Many of the transitions in the strongly correlated regions of the spectrum are bright. Both the optical response of silicon quantum dots and the high probabilities of producing a ME near $2E_g$ are a direct consequence of quantum confinement of strongly interacting electrons.

B. Quantum Dots with Defects. QDs are susceptible to impurities near the surface. Our calculations demonstrate that variances in the experimentally observed MEG rates and thresholds can be directly related to the presence of defects. Unlike molecules, in which a single missing atom or electron alters their chemical identity, nanocrystals retain inherent semiconducting properties with imperfections in the crystal and/or electronic structure. However, nanocrystal defects alter photoresponse properties due to the presence of new types of transitions. Diagrams of these transitions are displayed along the right-hand side of Figure 5. Spectral shifts appear for ionized species,[39] and a nonbonding valence behaves as a surface trap for charge carriers, reducing photoluminescence yields.[40]

A net positive or negative charge prior to photoabsorption significantly increases the MEG threshold of QDs. As an extreme example, cationic and anionic forms of Pb_4Se_4 do not photogenerate MEs at all. Contributions of the various transition types, including SE, ME, and intraband (IB), to the photoexcited states of anionic Pb_4Se_4 is displayed in Figure 5. The computed MEG threshold is higher in energy, $\sim 5E_g$, than the ionization threshold, removing all possibility of observing MEs in the photoexcited state. Excitons of cationic Pb_4Se_4 behave similarly,[38] where charging makes MEG energetically unattainable.

ME densities of charged silicon QDs are greatly reduced compared to the neutral.[37] The aforementioned differences in electronic structures between lead selenide and silicon are superseded by ionization, which reduces MEG in both weakly and strongly correlated systems. In comparison with the small model systems, much larger QDs, and particularly those with core/shell/ligand designs, will better compensate for excess charge through dielectric effects, and core atoms may be independent of charge localized to the surface. The effect of a dopant atom on the optical properties and MEG thresholds of semiconducting nanocrystals is similar to that of charge, since dopants introduce extra or missing electrons.[37]

Atomic vacancies on nanocrystal surfaces interfere with MEG, and the degree to which MEG is reduced depends on bonding properties of the electrons in the vicinity of the lattice defect. MEG thresholds are computed for model systems with nonbonding, selenium valence electrons, Pb_4Se_3, and nonbonding, lead valence electrons, Pb_3Se_4 (Figure 5). Transitions involving nonbonding selenium electrons dominate the excitation profile at low energy, as selenium electrons are energetically positioned within the band gap. Gap state (GS) transitions involving excess lead electrons are blue-shifted with respect to the selenium defect. Lead's valence electrons carry more angular momentum and are more shielded from nuclear attraction than valence electrons in selenium, allowing a certain flexibility for the reformation of chemical bonds. In this sense, excess lead on the surface is less detrimental to band structure than excess selenium. Likewise, the computed MEG threshold in Pb_4Se_3 is $2.6E_g$, which is identical to that of the pristine QD, and the MEG threshold in Pb_3Se_4 is $2.9E_g$. Surface deformities have a less severe effect on MEG thresholds than ionization, partly due to the self-healing nature of valence electrons.

Phonon-Induced Dephasing of Excitons

Excitons in QDs are coupled through interparticle Coulombic interactions and, as a result, are created in coherent
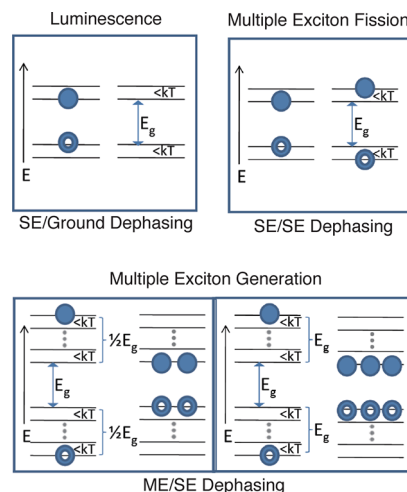

FIGURE 6. The upper left panel illustrates dephasing of a superimposed ground electronic state and a SE. The upper right panel shows dephasing two SEs, corresponding to MEF. Bottom panels show dephasing between SEs and MEs that contribute to ME generation.
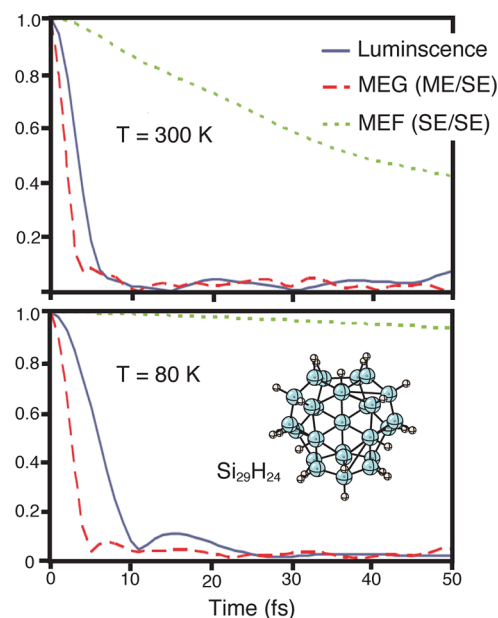

FIGURE 7. Decay of the exciton coherences involved in luminescence, MEG, and MEF in $Si_{29}H_{24}$.

superpositions. Due to coupling of excitons to phonons, the quantum coherence of these superpositions decays on a femtosecond time-scale.[41] Diagrams of the dephasing processes relevant to photoexcited QDs are given in Figure 6, computed dephasing functions[31] are shown in Figure 7, and corresponding dephasing times are presented in Table 1. The inverse of the lifetime of the superposition of the ground and first excited electronic states determines luminescence line width, allowing us to benchmark the calculations against experiment.[41] MEs become decorrelated from SEs soon

TABLE 1. Estimated Times (fs) of the Dephasing Processes Shown in Figure 6 in $Si_{29}H_{24}$ at 300 and 80 K

	pure dephasing times	
	300 K	80 K
luminescence (SE)	4.0 ± 0.1	7.0 ± 0.2
MEG (ME/SE)[a]	4.0 ± 0.1	7.3 ± 0.2
MEG (ME/SE)[b]	1.60 ± 0.05	2.96 ± 0.09
MEF (SE/SE)	54 ± 1	205.3 ± 0.9

[a]Coherence with the lowest energy biexciton, state energy = $2E_g$. [b]Coherence with the lowest energy triexciton, state energy = $3E_g$.

(<10 fs) after photoexcitation, at which point MEs can be detected experimentally. In this sense, MEG is facilitated by ultrafast ME/SE dephasing in QDs.

Once an ME state loses coherence with the initial photoexcited state, the ME decays into uncorrelated SEs, resulting in MEF. The phonon-induced pure dephasing process involved in MEF is an order of magnitude longer than pure dephasing involved in luminescence and MEG. This slower process of MEF involves orbitals that are energetically similar, and evolve coherently for longer periods of time than the energetically separated orbitals involved in the other two processes. Upon surpassing the dephasing times associated with MEG and MEF, excitons are no longer correlated through photoinduced coherences and evolve independently.

Temperature dependence in the dephasing rates results from anharmonicity in the ab initio potential energy surface. At higher temperatures, the nuclear lattice occupies higher vibrational states and, as a consequence, vibrational motion is more anharmonic. Furthermore, high temperature activates a broader spectrum of modes, including high-frequency phonons, which contributes to an increase in the electron−phonon coupling and faster dephasing. Low-frequency phonons are more susceptible to temperature effects, since a vibrational excitation requires relatively small amounts of thermal energy. MEF dephasing, dependent on low-frequency modes, exhibits large temperature dependence, whereas SE/ME dephasing is less sensitive to temperature effects given the dependence on high-frequency modes. Comparing dephasing times at 300 to 80 K, ME/SE dephasing is less than twice as fast at 300 K, whereas the rate of MEF increases nearly 4-fold.

Phonon-Assisted Exciton Dynamics

Model systems for the investigation of exciton multiplication by way of impact ionization[42,43] include Cd_6Se_6, Si_{10}, and $Si_{29}H_{24}$ (Figure 3). These three QDs differ in chemical composition, surface ligands (silicon hydrogenation), and size, all of which influence the rates of phonon-induced exciton
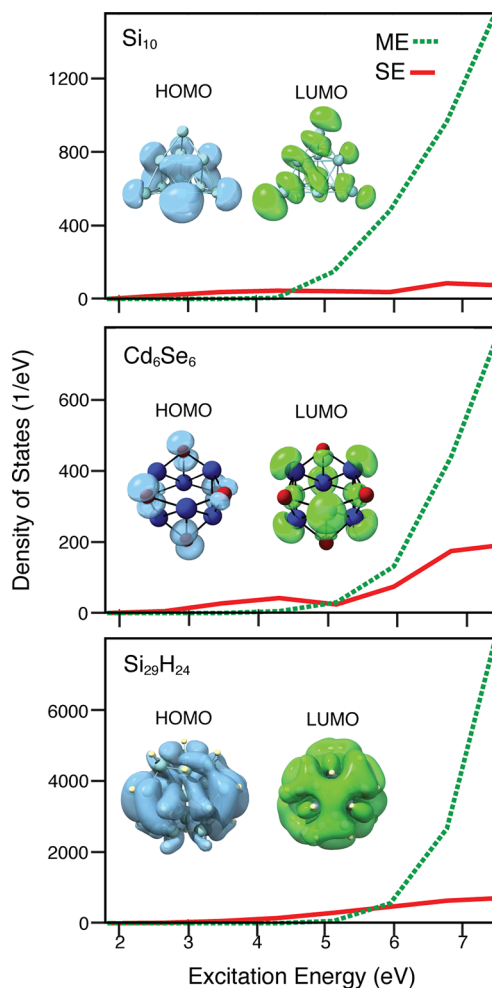
FIGURE 8. Densities of multiple exciton (ME) and single exciton (SE) states in Si_{10}, Cd_6Se_6, and $Si_{29}H_{24}$.

dynamics. A quantitative analysis of the relationship between physical attributes of QDs and MEG rates is determined. Densities of SEs and MEs are displayed in Figure 8. A large ME DOS indicates a high probability of exciton multiplication and, concomitantly, a rapid rate of impact ionization, provided that SEs and MEs are coupled through Coulomb and electron−phonon interactions.

ME populations of photoexcited Si_{10}, Cd_6Se_6, and $Si_{29}H_{24}$ are shown in Figure 9. The top panel compares MEG in Si_{10} and Cd_6Se_6, which are similar in size and, therefore, experience similar quantum confinement effects. The same amount of excess energy ($1.2E_g$) is delivered to each system, yet the silicon QD generates additional excitons at a faster rate than the cadmium selenide QD. Impact ionization rates depend on the phonon-induced coupling between SEs and MEs, which is attributed to the chemical composition of nanostructures, rather than size or incident energy alone.
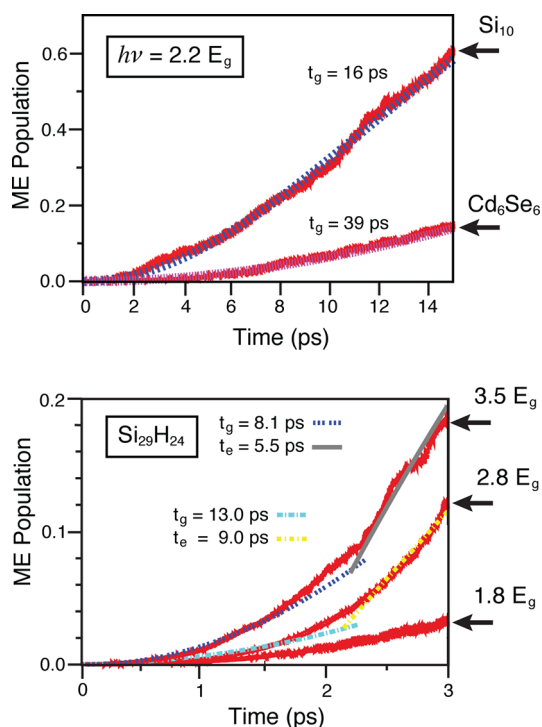
FIGURE 9. (top) Total population of the multiple exciton (ME) states following the initial excitation of a high-energy ($2.2E_g$) single exciton (SE) in Si_{10} and Cd_6Se_6. (bottom) ME populations in $Si_{29}H_{24}$ are shown, starting with SEs of energies, $3.5E_g$, $2.8E_g$, and $1.8E_g$.

Experimental studies have shown that MEG accelerates with increasing excitation energy.[13] Data recorded for initial excitation energies of $3.5E_g$, $2.8E_g$, and $1.8E_g$ in $Si_{29}H_{24}$ are shown in the bottom panel of Figure 9. Exciton multiplication is fastest at $3.5E_g$. From simple conservation of energy arguments, the MEG threshold is twice the amount of energy to create the lowest energy SE, that is, $2E_g$. However, since excitons are allowed to exchange energy with the lattice, SEs of energy below $2E_g$ generate additional excitons. At $1.8E_g$, exciton multiplication is extremely slow, yet possible. One can view this phonon-assisted MEG phenomenon as a result of excitons borrowing energy from the lattice, particularly from high-energy Si–H vibrations.

Many approaches to MEG in semiconducting nanocrystals assume exponential dynamics in order to construct a rate model based, for instance, on Fermi's golden rule.[22,26,27] Simulations presented here are carried out in the time-domain and do not require any assumptions as to the form of exciton multiplication dynamics. We find that the initial stage of MEG takes a Gaussian form in all three systems. This is a general observation, since at short times, the initial state couples to few other states, and quantum dynamics is Rabi-like. At long times, the dynamics involves a large ensemble of final states, and the evolution becomes exponential, as

described for instance by Fermi's golden rule. The exponential behavior is seen only in $Si_{29}H_{24}$, after a sufficient amount of time (about 2 ps) has passed for the dynamics to involve a large number of ME states. Smaller systems lack the sheer quantity of ME states to observe the transition from the Gaussian to exponential regime. We expect that in larger QDs, exponential dynamics required for a rate theory will dominate the MEG process; nevertheless, the initial step will remain Gaussian.

Summary

Central to the carrier multiplication process in semiconducting nanocrystals, the electron–electron Coulomb interaction correlates excitons and introduces finite probabilities of generating MEs from the absorption of a single photon. A strong Coulomb interaction allows for more efficient MEG, but is not a necessary requirement. For example, the Coulombic interaction in lead selenide QDs is highly screened, yet MEG does occur, as the excited state contains enough energy to support two largely independent excitons. For nanocrystalline silicon, in which electron–electron interactions are much more prominent, excitons are correlated and ME states appear at lower energies. Strong electron correlation is a mark of a material's ability to favorably distribute potential energy upon photoexcitation, and to lower the threshold for the coexistence of multiple electron–hole pairs.

The threshold for MEG is, however, of less consequence to the nanocrystal's ability to undergo impact ionization. MEG has been described in two forms, coherent[14,44] and incoherent.[27] Our methodology indicates incoherent impact ionization is an essential component to exciton multiplication, in which Coulombic interactions do not build long-lived dynamic coherences among SEs and MEs. Correlations between excitons, although a significant part of the initial photophysics, fade away quickly through interactions with the vibrating lattice. Qualitatively, impact ionization is driven by kinetic energy of hot excitons, and at high photoexcitation energies, kinetic energy is redistributed through either electron–phonon relaxation or Auger-type processes including impact ionization.

Photodriven exciton multiplication and subsequent phonon-induced pure-dephasing occur very rapidly in semiconductor QDs, followed by a competition between impact ionization and exciton thermalization. Figure 10 displays the exciton pathways in a QD over the initial 10 ps. The initial photoexcited state consists of a coherent superposition of SE and ME states. Interactions with the lattice destroy quantum mechanical coherences within tens of femtoseconds.
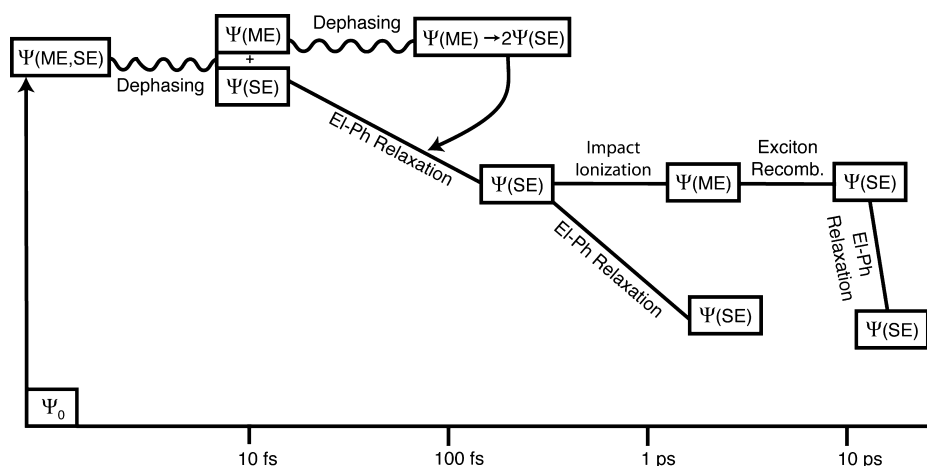
FIGURE 10. Quantum states comprised of MEs and SEs are generated upon absorbing photons of energies greater than $2E_g$. In the following 10 fs, quantum coherences between MEs and SEs are destroyed. High-energy excitons produce additional MEs by incoherent impact ionization, and exciton lose energy through electron—phonon interactions. At 10 ps after photoexcitation, MEs can undergo Auger recombination, regenerating high-energy excitons.

As energy flows from the electronic degrees of freedom, finite probabilities exist for the creation of additional excitons via impact ionization. The system returns to the band edge exciton within 10 ps.

Our techniques, including many-electron wave functions and nonadiabatic electron—phonon dynamics, are limited to model systems. The conclusions obtained with model nanoclusters apply qualitatively to realistic QDs, since exciton multiplication ultimately depends on microscopic quantum properties. When extrapolating results from model systems to larger crystals, one needs to consider several factors, including the scaling of the Coulomb interaction with electron—hole separation distance, the surface to volume ratio, and changes in the DOS and electron—phonon coupling with QD size. MEG simulations carried out with small QDs indicate that photodriven MEG is very efficient and that the complementary process of SE/ME dephasing occurs on a 10—100 fs time-scale. Additionally, electron—phonon energy exchange requires 100—1000 fs and is greatly facilitated by surface ligands. Impact ionization takes place on a picosecond time scale. The MEG yields and thresholds are strongly affected by surface defects. In comparison, exciton multiplication in bulk semiconductors does not occur readily from photoexcitation, requires more time, and is largely independent of surface properties.

Exciton multiplication provides a clear benefit to photovoltaic technology. The realization of QD solar cells achieving next generation standards, however, is still in progress. First principle simulations provide unbiased evidence for the existence of exciton multiplication in QDs, a formalism in which to describe the mechanism of MEG, and a clear understanding as to why certain nanocrystals multiply excitons better than others do.

BIOGRAPHICAL INFORMATION

Heather M. Jaeger graduated from Indiana University Purdue University at Indianapolis in 2006 with a degree in Chemistry. She obtained her Ph.D. in 2010 under Henry Schaefer at the University of Georgia, before joining Gregory Tschumper's group at the University of Mississippi. Since 2011, she has been working in the Prezhdo group at the University of Rochester, where her research focus has been the characterization of electronic excitation in condensed phases.

Kim Hyeon-Deuk received a Bachelor's degree in Statistical Physics in 1999 and a Master's degree in Theoretical Physics in 2001 from Kyoto University. He finished his Ph.D. with Hisao Hayakawa at Kyoto University in 2004. He joined the chemistry department of Kyoto University in 2007, where his research interests include developing new simulation methods based on physical principles and applying them to quantum dissipation systems.

Oleg V. Prezhdo obtained a Diploma in Theoretical Chemistry in 1991 from Kharkiv National University, Ukraine, under Anatoly Luzanov. He completed his Ph.D. with Peter Rossky at the University of Texas, Austin. After a postdoctoral fellowship with John Tully at Yale University, he joined the chemistry department at the

University of Washington in 1998, achieving Associate and Full Professor in 2002 and 2005, respectively. In 2008, he was elected Fellow of the American Physical Society and in 2010 was offered Senior Professorship at the University of Rochester. Since 2008, he has served as editor for *The Journal of Physical Chemistry,* since 2011 as editor for *The Journal of Physical Chemisty Letters,* and since 2013 as editor for *Surface Science Reports*. A recipient of multiple national and international awards, he held invited professorships in France, Germany, and Japan. His current research interests range from fundamental aspects of semiclassical physics, to excitation dynamics in nanoscale and biological systems.

FOOTNOTES

*To whom correspondence should be addressed.
The authors declare no competing financial interest.

REFERENCES

1 Alivisatos, A. P. Semiconductor clusters, nanocrystals, and quantum dots. *Science* **1996**, *271*, 933–937.

2 Efros, A. L.; Rosen, M. The Electronic Sructure of Semiconductor Nanocrystals. *Annu. Rev. Mater. Sci.* **2000**, *30*, 475–521.

3 Steigerwald, M. L.; Brus, L. Synthesis, Stabilization, and Electronic Structure of Quantum Semiconductor Nanoclusters. *Annu. Rev. Phys. Chem.* **1989**, *19*, 471–495.

4 Nozik, A. J.; Beard, M. C.; Luther, J. M.; Law, M.; Ellingson, R. J.; Johnson, J. C. Semiconductor Quantum Dot and Quantum Dot Arrays and Applications of Multiple Exciton Generation to Third-Generation Photovoltaic Solar Cells. *Chem. Rev.* **2010**, *110*, 6873–6890.

5 Nozik, A. J. Quantum dot solar cells. *Phys. E* **2002**, *14*, 115–120.

6 Zhu, X.-Y. Charge-Transfer Excitons at Organic Semiconductor Surfaces and Interfaces. *Acc. Chem. Res.* **2009**, *42*, 1779–1787.

7 Steigerwald, M. L.; Brus, L. E. Semiconductor Crystallites: A Class of Large Molecules. *Acc. Chem. Res.* **1990**, *23*, 183–188.

8 Prezhdo, O. V. Photoinduced Dynamics in Semiconductor Quantum Dots: Insights from Time-Domain ab initio Studies. *Acc. Chem. Res.* **2009**, *42*, 2005–2016.

9 Grundmann, M.; Christen, J.; Ledentsov, N. N.; Böhrer, J.; Bimberg, D.; Ruvimov, S. S.; Werner, P.; Richter, U.; Gösele, U.; Heydenreich, J.; Ustinov, V. M.; Egorov, A. Y.; Zhukov, A. E.; Kopev, P. S.; Alferov, Z. I. Ultranarrow Luminescence Lines from Single Quantum Dots. *Phys. Rev. Lett.* **1995**, *74*, 4043–4046.

10 Marzin, J.-Y.; Gérard, J.-M.; Izraël, A.; Barrier, D. Photoluminescence of Single InAs Quantum Dots Obtained by Self-Organized Growth on GaAs. *Phys. Rev. Lett.* **1994**, *73*, 716–719.

11 Luo, J.-W.; Franceschetti, A.; Zunger, A. Carrier Multiplication in Semiconductor Nanocrystals: Theoretical Screening of Candidate Materials Based on Band-Structure Effects. *Nano Lett.* **2008**, *8*, 3174–3181.

12 Beard, M. C. Multiple Exciton Generation in Semiconductor Quantum Dots. *J. Phys. Chem. Lett.* **2011**, *2*, 1282–1288.

13 Schaller, R. D.; V. I., K. High efficiency carrier multiplication in PbSe nanocrystals: Implications for solar energy conversion. *Phys. Rev. Lett.* **2004**, *92*, 186601.

14 Ellingson, R. J.; Beard, M. C.; Johnson, J. C.; Yu, P.; Micic, O. I.; Nozik, A. J.; Shabaev, A.; Efros, A. L. Highly Efficient Multiple Exciton Generation in Colloidal PbSe and PbS Quantum Dots. *Nano Lett.* **2005**, *5*, 865–871.

15 Trinh, M. T.; Houtepen, A. J.; Schins, J. M.; Hanrath, T.; Piris, J.; Knulst, W.; Goossens, A. P. L. M.; Siebbeles, L. D. A. In Spite of Recent Doubts Carrier Multiplication Does Occur in PbSe Nanocrystals. *Nano Lett.* **2008**, *8*, 1713–1718.

16 Schaller, R. D.; M., S.; Pietryga, J. M.; V., I. Klimov Seven excitons at a cost of one: Redefining the limits for conversion efficiency of photons into charge carriers. *Nano Lett.* **2006**, *6*, 424–429.

17 Murphy, J. E.; Beard, M. C.; Norman, A. G.; Ahrenkiel, S. P.; Johnson, J. C.; Yu, P.; Micic, O. I.; Ellingson, R. J.; Nozik, A. J. PbTe Colloidal Nanocrystals: Synthesis, Characterization, and Multiple Exction Generation. *J. Am. Chem. Soc.* **2006**, *128*, 3241–3247.

18 Beard, M. C.; Knutsen, K. P.; Yu, P.; Luther, J. M.; Song, Q.; Metzger, W. K.; Ellingson, R. J.; Nozik, A. J. Multiple Exciton Generation in Colloidal Silicon Nanocrystals. *Nano Lett.* **2007**, *7*, 2506–2512.

19 Trinh, M. T.; Limpens, R.; de Boer, W. D. A. M.; Schins, J. M.; Siebbeles, L. D. A.; Gregorkiewicz, T. Direct generation of multiple excitons in adjacent silicon nanocrystals revealed by induced absorption. *Nat. Photonics* **2012**, *6*, 316–321.

20 Nail, G.; Chang, L.-Y.; Geyer, S. M.; Bawendi, M. G. Perspective on the Prospects of a Carrier Mutiplication Nanocrystal Solar Cell. *Nano Lett.* **2011**, *11*, 2145–2151.

21 McGuire, J. A.; Joo, J.; Pietryga, J. M.; Schaller, R. D.; Klimov, V. I. New aspects of carrier multiplication in semiconductor nanocrystals. *Acc. Chem. Res.* **2008**, *41*, 1810–1819.

22 Piryatinski, A.; Velizhanin, K. A. An exciton scattering model for carrier multiplication in semiconductor nanocrystals: Theory. *J. Chem. Phys.* **2010**, *133*, 084508.

23 Miaja-Avila, L.; Tritsch, J. R.; Wolcott, A.; Chan, W.-L.; Nelson, C. A.; Zhu, X.-Y. Direct Mapping of Hot-Electron Relaxation and Multiplication Dynamics in PbSe Quantum Dots. *Nano Lett.* **2012**, *12*, 1588–1591.

24 Klimov, V. I. Mechanisms for Photogeneration and Recombination of Multiexcitons in Semiconductor Nanocrystals: Implications for Lasing and Solar Energy Conversion. *J. Phys. Chem. B* **2006**, *110*, 16827–16845.

25 Cho, B.; Peters, W. K.; Hill, R. J.; Courtney, T. L.; Jonas, D. M. Bulklike Hot Carrier Dynamics in Lead Sulfide Quantum Dots. *Nano Lett.* **2010**, *10*, 2498–2505.

26 Rabani, E.; Baer, R. Theory of multiexciton generation in semiconductor nanocrystals. *Chem. Phys. Lett.* **2010**, *496*, 227–235.

27 Franceschetti, A.; An, J. M.; Zunger, A. Impact ionization can explain carrier multiplication in PbSe quantum dots. *Nano Lett.* **2006**, *6*, 2191–2195.

28 Beard, M. C.; Midgett, A. G.; Hanna, M. C.; Luther, J. M.; Hughes, B. K.; Nozik, A. J. Comparing Multiple Exciton Generation in Quantum Dots to Impact Ionization in Bulk Semiconductors: Implications for Enhancement of Solar Energy Conversion. *Nano Lett.* **2010**, *10*, 3019–3027.

29 Sambur, J. B.; Novet, T.; Parkinson, B. A. Multiple Exciton Collection in a Sensitized Photovoltaic System. *Science* **2010**, *330*, 63–66.

30 Semonin, O. E.; Luther, J. M.; Choi, S.; Chen, H.-Y.; Gao, J.; Nozik, A. J.; Beard, M. C. Peak External Photocurrent Quantum Efficiency Exceeding 100% via MEG in a Quantum Dot Solar Cell. *Science* **2011**, *334*, 1530–1533.

31 Mukamel, S. *Principles of Nonlinear Optical Spectroscopy*; Oxford University Press: New York, 1995; pp 543—550.

32 Hyeon-Deuk, K.; Madrid, A. B.; Prezhdo, O. V. Symmetric band structures and asymmetric ultrafast electron and hole relaxations in silicon and germanium quantum dots: time-domain ab initio simulation. *Dalton Trans.* **2009**, *45*, 10069–10077.

33 Kilina, S. V.; Kilin, D. S.; Prezhdo, O. V. Breaking the Phonon Bottleneck in PbSe and CdSe Quantum Dots: Time-Domain Density Functional Theory of Charge Carrier Relaxation. *ACS Nano* **2009**, *3*, 93–99.

34 Isborn, C. M.; Kilina, S. V.; Li, X.; Prezhdo, O. V. Generation of Multiple Excitons in PbSe and CdSe Quantum Dots by Direct Photoexcitation: First-Principles Calculations on Small PbSe and CdSe Clusters. *J. Phys. Chem. C* **2008**, *112*, 18291–18294.

35 Idrobo, J. C.; Halabica, A.; Magruder, R. H., III; Haglund, R. F., Jr.; Pennycook, S. J.; Pantelides, S. T. Universal optical response of Si-Si bonds and its evolution from nanoparticles to bulk crystals. *Phys. Rev. B* **2009**, *79*, 125332.

36 Fischer, S. A.; Madrid, A. B.; Isborn, C. M.; Prezhdo, O. V. Multiple Exciton Generation in Small Si Clusters: A HIgh-Level, Ab Initio Study. *J. Phys. Chem. Lett.* **2009**, *1*, 232–237.

37 Fischer, S. A.; Isborn, C. M.; Prezhdo, O. V. Excited states and optical absorption of small semiconducting clusters: Dopants, defects, and charging. *Chem. Sci.* **2011**, *2*, 400–406.

38 Isborn, C. M.; Prezhdo, O. V. Charging Quenches Multiple Exciton Generation in Semiconductor Nanocrystals: First-Principles Calculations on Small PbSe Clusters. *J. Phys. Chem. C* **2009**, *113*, 12617–12621.

39 Franceschetti, A.; Zunger, A. Optical transitions in charged CdSe quantum dots. *Phys. Rev. B* **2000**, *62*, R16287–R16290.

40 Jones, M.; Lo, S. S.; Scholes, G. D. Quantitative modeling of the role of surface traps in CdSe/CdS/ZnS nanocrystal photoluminescence decay dynamics. *Proc. Nat. Acad. Sci. U.S.A.* **2009**, *106*, 3011–3016.

41 Madrid, A. B.; Hyeon-Deuk, K.; Habenicht, B. F.; Prezhdo, O. V. Phonon-Induced Dephasing of Excitons in Semiconductor Quantum Dots: Multiple Exciton Generation, Fission, and Luminescence. *ACS Nano* **2009**, *3*, 2487–2494.

42 Hyeon-Deuk, K.; Prezhdo, O. V. Multiple Exciton Generation and Recombination Dynamics in Small Si and CdSe Quantum Dots: An Ab Initio Time-Domain Study. *ACS Nano* **2012**, *6*, 1239–1250.

43 Hyeon-Deuk, K.; Prezhdo, O. V. Time-Domain ab initio Study of Auger and Phonon-Assisted Auger Processes in a Semiconductor Quantum Dot. *Nano Lett.* **2011**, *11*, 1845–1850.

44 Shabaev, A.; Efros, A. L.; Nozik, A. J. Multiexciton Generation by a Single Photon in Nanocrystals. *Nano Lett.* **2006**, *6*, 2856–2863.